

Resonant Photoelectron Diffraction with circularly polarized light

Martin Morscher,¹ Frithjof Nolting,² Thomas Brugger,¹ and Thomas Greber^{1,*}

¹*Physik-Institut, Universität Zürich, Winterthurerstrasse 190, CH-8057 Zürich, Switzerland*

²*Paul Scherrer Institut, CH-5232 Villigen PSI, Switzerland*

(Dated: October 18, 2018)

Resonant angle scanned x-ray photoelectron diffraction (RXPD) allows the determination of the atomic *and* magnetic structure of surfaces and interfaces. For the case of magnetized nickel the resonant L_2 excitation with circularly polarized light yields electrons with a dichroic signature from which the dipolar part may be retrieved. The corresponding L_2MM and L_3MM Auger electrons carry different angular momenta since their source waves rotate the dichroic dipole in the electron emission patterns by distinct angles.

PACS numbers: 79.60.-i, 61.05.js, 75.25.-j, 79.60.Bm

Keywords: Resonant Photoemission, XPD, Dichroism

The quest for atomic scale structure determination at surfaces and interfaces lead to the development of a large number of powerful methods [1]. Among those, x-ray photoelectron spectroscopy (XPS) with angular resolution (XPD) allows structure determination paired with chemical and magnetic sensitivity [2]. The signal is best, when the x-ray absorption coefficient is at maximum. These maxima occur in resonant excitation and have so far been exploited for the probing of defect states in TiO_2 [3], for looking inside an endofullerene [4], or for the investigation of the mixed valence structure of magnetite [5].

In this letter, angle scanned resonant photoelectron diffraction (RXPD) is applied to nickel, the "fruit fly" of resonant photoemission [6–10]. Circularly polarized light is used for the precise measurement of the dipole induced by the x-ray magnetic circular dichroism which is largest at resonance. After this proof of principle we show that the angular momentum of the outgoing electrons can be measured with RXPD. This extends the results of Daimon et al., who demonstrated that forward scattering XPD patterns rotate due to the angular momentum of circularly polarized photons [11–13]. Here, the electron source wave [14, 15] rotates the magnetisation direction in the final state of the emitted electrons. It is also found that Auger electrons may carry angular momenta opposite to that of the exciting photon and larger than \hbar .

Circular magnetic dichroism ΔI_{MD} is the difference between the absorption coefficient of right and left circularly polarized light. It is proportional to the scalar product of the magnetization \mathbf{m} and the angular momentum of the incoming photon \mathbf{L}_{ph} [16].

$$\Delta I_{MD} \propto \mathbf{m} \cdot \mathbf{L}_{ph} \quad (1)$$

For right circularly polarized light (σ^+) \mathbf{L}_{ph} is parallel to the propagation direction of the photon, and for left circularly polarized light (σ^-) \mathbf{L}_{ph} is antiparallel. ΔI_{MD} is a dipole, i.e. proportional to $\cos(\vartheta)$, where ϑ is the angle between \mathbf{m} and \mathbf{L}_{ph} . From this follows that the absolute orientation of \mathbf{m} is determined from three or

more non-coplanar light incidences.

Photoemission yields ΔI_{MD} , under the assumption that the photoemission current is proportional to the x-ray absorption coefficient. This must not hold for partial measurements like in angular resolved photoemission where $dI/d\Omega$ is measured [17]. The different photoelectron source waves of electrons excited with differently polarized light lead to different photoemission final states that comprise information on the magnetism *and* the surrounding of the emitter [18]. Here we show that contributions of the atomic and the magnetic structure can be disentangled with a spin integrated experiment.

The experiments have been performed at the SIM beamline at the Swiss Light Source (SLS) [19] in an end-station dedicated for x-ray photoelectron spectroscopy (XPS) and angle-resolved x-ray photoelectron diffraction (XPD) with a base pressure below $2 \cdot 10^{-10}$ mbar. The x-rays impinge perpendicular to the polar rotation axis with an angle θ_o between the x-rays and the electron energy analyzer of 55° (see Figure 1). The degree of polarization is better than 98%. All measurements are done at room temperature. The Ni(111) yoke crystal [20] was cleaned by repeated cycles of argon sputtering and annealing. It is magnetized by passing a current of 2 A for 30 s through the yoke coil. The resulting magnetization was inferred from an x-ray magnetic circular dichroism (XMCD) spectrum at the Ni L_2, L_3 -edges in the total-electron-yield mode. Comparison with corresponding spectra of Chen et al. [21] indicate a magnetization of $\sim 40\%$, which is not 100 % due to a multidomain structure.

Resonant photoemission on 3d transition metals is most intense at the L_3 absorption edge [3, 21]. Here we investigate the L_2 resonance since it provides L_2MM *and* L_3MM emission which allows for direct comparison and consistency checks. Figure 2 shows resonant x-ray photoelectron spectra from magnetized Ni(111) of right and left circularly polarized light. The photon energy is set on the Ni L_2 -resonance ($2p_{1/2} \rightarrow 3d$) at $\hbar\omega = 870.5$ eV. The Fermi level E_F at 870.5 eV electron energy, the L_2MM

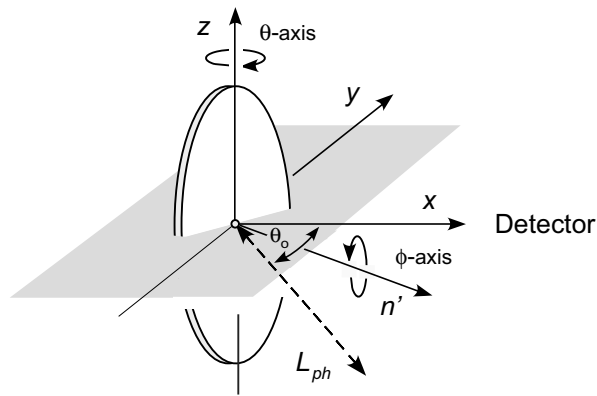


FIG. 1: Geometry of the XPD experiment. The electron detection is parallel to x and the polar (θ) rotation axis parallel to z . The sample normal \mathbf{n}' is the azimuthal (ϕ) rotation axis and lies with the light incidence along its angular momentum \mathbf{L}_{ph} in the xy plane (shaded area), $\theta_o = 55^\circ$ away from x .

(863.8 eV) 6 eV satellite (see [22] and references therein), and the L_3MM (846.2 eV) Auger deexcitation peak are most prominent. The spectra have been normalized with the photon flux. Figure 2b) demonstrates circular dichroism in these resonantly excited electron emission spectra. The asymmetry $A = (I(\sigma^+) - I(\sigma^-))/(I(\sigma^+) + I(\sigma^-))$ between right and left circularly polarized light exhibits a maximum at α_2 and a minimum at α_3 . The asymmetry can be reversed by switching the magnetization or by the rotation of the sample by 180° [23]. Off resonance, at $\hbar\omega = 873.5$ eV the dichroic asymmetry in the L_2MM Auger line is $1.4 \pm 0.8\%$ (data not shown). The extrema α_2 at 848.4 eV and α_3 at 863.6 eV do not exactly coincide with the L_2MM and the L_3MM intensity maxima, which indicates multiplet structure [24]. In the following we use the labels α_i^σ for electrons at the energies of α_2 and α_3 , excited with σ^+ and σ^- polarized radiation, respectively.

If we perform on these resonances angle scanned x-ray photoelectron diffraction (RXPD), the experiment yields information on the atomic *and* the magnetic structure. Briefly, the sample frame (x', y', z') is rotated in the lab frame (x, y, z). The photoelectron intensity I is mapped in polar coordinates ($f(\theta, \phi)$), where the polar angle θ and the azimuthal angle ϕ define the sample orientation with respect to the electron detection direction (see Figure 1) [25]. This leads to ΔI_{MD} to a dipolar function $D(\theta, \phi)$ in the XPD map that depends on \mathbf{L}_{ph} , the electron detection direction in the lab frame and $\mathbf{m}'(\theta_m, \phi_m, a_m)$ in the sample frame, where the amplitude a_m is a measure for the magnitude of the dichroism [23].

Figure 3a) shows RXPD data for α_2^+ . The XPD map is dominated by the information on the atomic structure which corresponds to that of a face centered cubic (*fcc*) crystal which is cut along the (111) plane [26]. Below

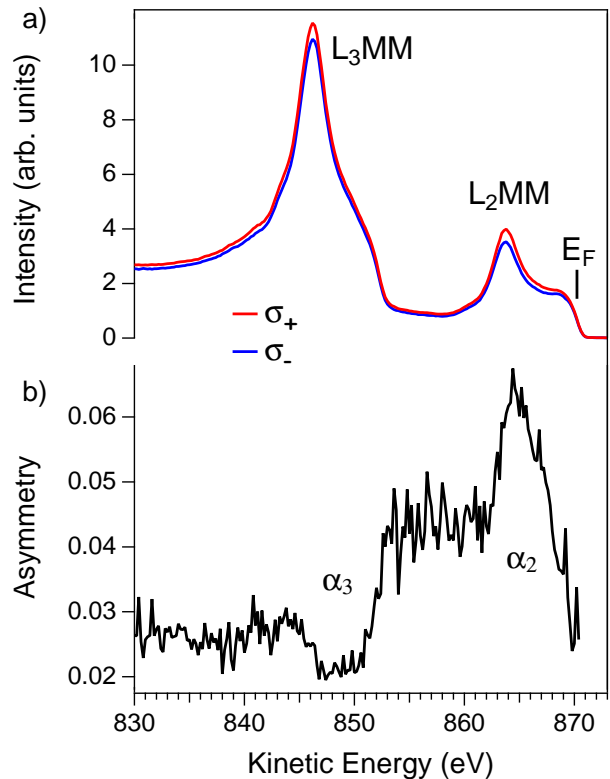


FIG. 2: (Color online) (a) Near normal photoelectron spectra with left and right circularly polarized light with an angle of 30° and $180-30^\circ$ between \mathbf{L}_{ph} and \mathbf{m}' . The photon energy is set on the Ni L_2 -resonance at $\hbar\omega = 870.5$ eV. The spectra have been normalized with the photon flux. The Fermi level E_F , the L_2MM and the L_3MM Auger deexcitation peaks are indicated. (b) The asymmetry A between right and left circularly polarized light exhibits two distinct extrema α_2 and α_3 , on which we performed XPD measurements.

the obvious atomic structure dichroic information must be hidden. In order to visualize the dichroism, we form the asymmetry A between the α_2^+ and the α_2^- XPD scans (see Figure 3b). These data contain information on the dipolar (magnetic) nature of dichroism and higher order multipoles, which are related to differences in the diffraction patterns due to different source waves [11, 27]. The dipolar part has the symmetry $A(\theta, \phi) = -A(\theta, \phi + 180^\circ)$, as it is expected for in plane magnetisation. Figure 3c) shows the fit of a dipolar function $D(\theta, \phi)$, which determines \mathbf{m}' . We find $\theta_m = 89.0 \pm 1^\circ$, and $\phi_m = 39.1 \pm 1^\circ$, where $\phi = 0$ is set to the $[\bar{1}10]$ direction. This result is consistent with spin polarized photoemission [20], though the magnetization is not aligned along the second easy axis $[\bar{1}10]$ as it was the case for an other Ni(111) picture frame crystal [28]. The rotation of the sample and the incidence of the light impose on D two nodal lines ($\mathbf{m}' \cdot \mathbf{L}_{ph} = 0$): A circle at $\theta_o = 55^\circ$, and a diameter perpendicular to ϕ_m . In Figure 3d) the residuum of the asymmetry and D is shown. It has the C_3 symmetry

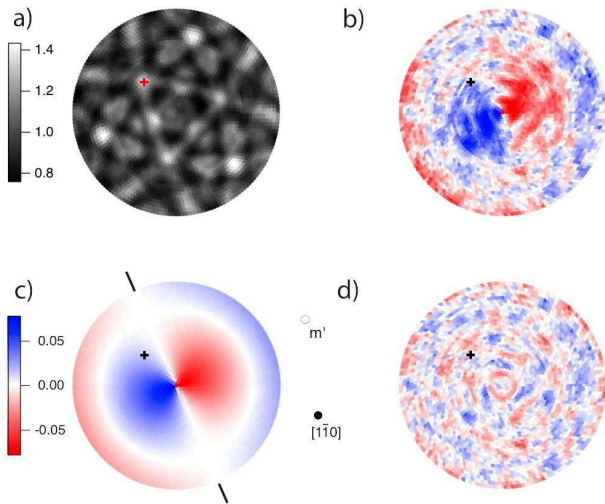


FIG. 3: (Color online) (a) Resonant x-ray photoelectron diffraction (RXPD) data of Ni(111). The 3500 stereographically projected data points for polar angles $0 \leq \theta \leq 70^\circ$ of the intensity at α_2 ($E_{kin}=863.8$ eV, $\hbar\omega = 870.5$ eV, σ^+) in Figure 2. The data are ϕ -averaged, i.e. normalized at each polar angle with the corresponding average intensity. (b) Asymmetry of two XPD data sets at α_2 measured with right and left circularly polarized light. The twofold i.e. dipolar pattern reveals the direction of the magnetization. (c) D -function-fit to the asymmetry in (b). The direction of magnetisation \mathbf{m}' and ticks for the corresponding azimuthal orientation at $\phi_m \pm 90^\circ$ are indicated. The [011]-direction (cross), and the yoke axis along $[1\bar{1}0]$ are marked. (d) Residuum of the fit in (c) with respect to (b).

of the substrate and indicates further differences in the diffraction patterns due to different source waves created by σ^+ and σ^- photons, respectively. Such effects have been pioneered by Daimon et al., where they showed that the angular momenta of the photons are transferred to the photoelectrons, which in turn lead to an emitter scatterer distance dependent rotation of the forward scattering peak [11, 12].

For the data in Figure 3 b) we expect no photon induced rotation because in the asymmetry between σ^+ and σ^- any such effect should be canceled. This changes, when a dipolar function D is fitted to an individual XPD scan with either σ^+ or σ^- radiation. If we fit a dipolar function D to the data in Figure 3a), or the ones recorded with σ^- polarization, we find magnetisation directions which are within $\pm 6^\circ$ consistent with the magnetization direction as found from Figure 3 b). Although this has the practical advantage that the magnetization is determined without switching the light polarization, it is not very accurate since the D -function is much weaker than the forward scattering induced XPD patterns.

If we want to extract more quantitative information on the rotation of the D -functions upon use of photons with plus or minus \hbar angular momentum we have to perform a

normalisation that removes the forward scattering intensity modulations but preserves, in contrast to the asymmetry used in Figure 3 the angular momentum of σ^+ or σ^- . We do so in using the ϕ -averaged data $\bar{\alpha}_i^\sigma$ and form $\Delta\alpha_2^\sigma = 2 \cdot \bar{\alpha}_2^\sigma / (\bar{\alpha}_3^+ + \bar{\alpha}_3^-) - 1$ and vice versa.

As α_2 and α_3 electrons are expected to have very similar XPD patterns [15] - the wavelength-difference between the two selected electron energies of α_2 and α_3 is 1% - most XPD information on the atomic structure should be cancelled, though the $\Delta\alpha_i^\sigma$ are expected to show a polarization dependent rotation $\Delta\phi_m(\alpha_i, \sigma)$ of the observed magnetisation direction. For the 6 eV satellite, i.e. L_2MM transition, we find a rotation $\Delta\phi_m$ of $\pm 4.2^\circ$ around the value of Figure 3b). It is related to the Daimon effect, i.e. forward scattering peak rotation [11]. Essentially, the angular momentum of an outgoing photoelectron induces a rotation of all features in the XPD patterns with respect to the crystal lattice. For single scattering the maximum angle of rotation γ_{max} is given by $n \cdot \hbar / (R \cdot p \cdot \sin^2(\theta_o))$, where R is the distance between emitter and scatterer, p the momentum of the outgoing electron and θ_o the angle between the light incidence and the electron detection (see Figure 1) [12, 29]. For nickel, $n = 1$, an electron kinetic energy of 850 eV and $\theta_o = 55^\circ$, γ_{max} gets 2.2° . Of course, the angular shift is not isotropic, it depends on the angle between the electron angular momentum and the nearest neighbour directions. However, for an *fcc* material as it is nickel, the 12 nearest neighbours of an emitter in the bulk sit on a sphere with radius R , on the vertices of a cuboctahedron and must lead to a fairly isotropic rotation of the XPD patterns around the axis of the incoming photons. The $\Delta\phi_m(\alpha_2)$'s have the same sense of rotation as the corresponding photon angular momentum and are compatible with the transfer of $2\hbar$ of angular momentum to the emitted electrons.

Figure 4 shows the $\Delta\alpha_2^\sigma$ and the $\Delta\alpha_3^\sigma$ XPD scans for σ^+ and σ^- radiation. Dipolar functions (D) as shown in Figure 3c) appear, where the sign changes upon change of the polarization. The D -functions for $\Delta\alpha_2^\pm$ and $\Delta\alpha_3^\pm$ indicate $\Delta\phi_m$'s of $\pm 4.2^\circ$ and $\mp 12.6^\circ$, respectively. We want to note that the use of more than 3000 different photon incidence angles allows a very accurate $\pm 0.8^\circ$ determination of the $\Delta\phi_m(\alpha_2)$'s and permits for single quantum assignments $2\hbar$ ($-2\hbar$). In the $\Delta\alpha_3$ patterns with a lower asymmetry (see Figure 2) the error increases by a factor of 3 and makes it compatible with angular momenta of $-6 \pm 2\hbar$ or $6 \pm 2\hbar$ (see Figure 4 e)). This surprising result implies that a L_3MM Auger electron channel produces electrons with large, opposite angular momentum compared to that of the photons. These results emphasise that the information on the angular momentum of an electron source wave may not only be accessed by a forward scattering peak rotation [11], but for magnetic systems also by the precise measurement of the source wave dependent circular magnetic dichroism.

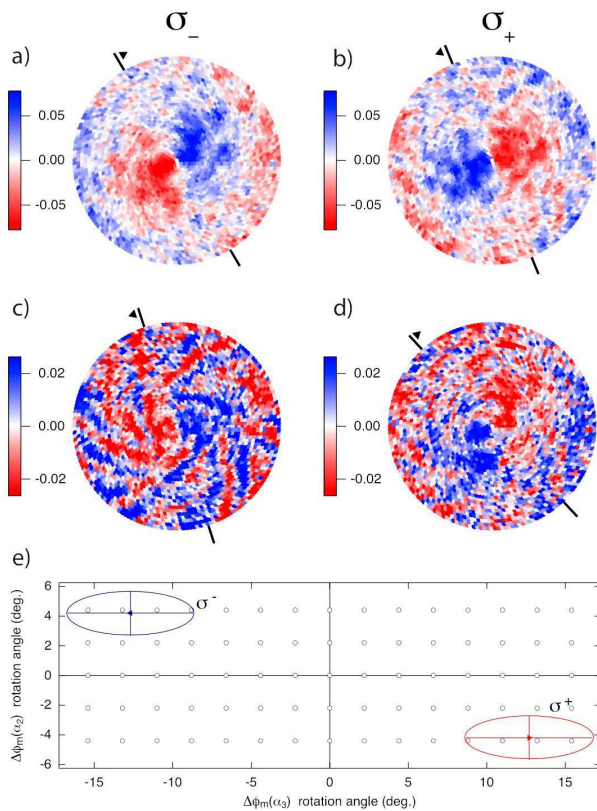


FIG. 4: (Color online) (a)-(d): Individual XPD patterns with the same orientation as in Figure 3 of (a) $\Delta\alpha_2^-$, (b) $\Delta\alpha_2^+$, (c) $\Delta\alpha_3^-$ and (d) $\Delta\alpha_3^+$ (for definition see text). The ticks lie on the azimuth of the node of the corresponding dichroic dipole. The solid triangles indicate the rotation towards the magnetisation direction. (e) Rotation angles $\Delta\phi_m(\alpha_2^\pm)$ versus $\Delta\phi_m(\alpha_3^\pm)$. For a given polarization the electrons rotate in opposite directions. The ellipses represent the error bars. The open circles are the rotation angles as expected from quantized angular momenta $n \cdot \hbar$.

In summary it has been shown that resonant x-ray photoelectron diffraction (RXPD) is suited to extract the atomic and magnetic structure of surfaces and interfaces. Furthermore it is demonstrated that the method directly accesses the angular momenta of the emitted electrons.

Fruitful discussions with J. Osterwalder and the support of the Swiss National Science Foundation are gratefully acknowledged. The experiments have been performed at the Swiss Light Source.

* Electronic address: greber@physik.uzh.ch

[1] M. A. Van Hove, *Surface and Interface Analysis* **28**, 36 (1999).
 [2] C. S. Fadley, *Journal of Electron Spectroscopy and Related Phenomena* **178**, 2 (2010).
 [3] P. Krüger, S. Bourgeois, B. Domenichini, H. Magnan, D. Chandesris, P. Le Fèvre, A. Flank, J. Jupille, L. Flo-

reano, A. Cossaro, et al., *Physical Review Letters* **100**, 055501 (2008).
 [4] M. Treier, P. Ruffieux, R. Fasel, F. Nolting, S. Yang, L. Dunsch, and T. Greber, *Physical Review B* **80**, 081403 (2009).
 [5] H. Magnan, P. Le Fevre, D. Chandesris, P. Kruger, S. Bourgeois, B. Domenichini, A. Verdini, L. Floreano, and A. Morgante, *Physical Review B* **81**, 085121 (2010).
 [6] C. Guillot, Y. Ballu, J. Paignè, J. Lecante, K. Jain, P. Thiry, R. Pinchaux, Y. Pètroff, and L. Falicov, *Physical Review Letters* **39**, 1632 (1977).
 [7] L. A. Feldkamp and L. C. Davis, *Physical Review Letters* **43**, 151 (1979).
 [8] L. Tjeng, C. Chen, P. Rudolf, and G. Meigs, *Physical Review B* **48**, 13378 (1993).
 [9] G. van der Laan, *International Journal of Modern Physics B* **8**, 641 (1994).
 [10] M. Weinelt, A. Nilsson, M. Magnuson, T. Wiell, A. Wassdahl, O. Karis, A. Föhlisch, N. Mårtensson, J. Stöhr, and M. Samant, *Physical Review Letters* **78**, 967 (1997).
 [11] H. Daimon, T. Nakatani, S. Imada, S. Suga, Y. Kagoshima, and T. Miyahara, *Japanese Journal of Applied Physics Part 2 - Letters* **32**, L1480 (1993).
 [12] H. Daimon, *Physical Review Letters* **86**, 2034 (2001).
 [13] F. Matsui, T. Matsushita, and H. Daimon, *Journal of Electron Spectroscopy and Related Phenomena* **178**, 221-240 (2010).
 [14] T. Greber, J. Osterwalder, S. Hufner, and L. Schlapbach, *Physical Review B* **45**, 4540 (1992).
 [15] T. Greber, J. Osterwalder, D. Naumovic, A. Stuck, S. Hufner, and L. Schlapbach, *Physical Review Letters* **69**, 1947 (1992).
 [16] J. Stöhr and H. Siegmans, *Magnetism - From Fundamentals to Nanoscale Dynamics* (Springer, 2006).
 [17] C. Westphal, J. Bansmann, M. Getzlaff, and G. Schönhense, *Physical Review Letters* **63**, 151 (1989).
 [18] A. Chassé, W. Kuch, M. Kotsugi, X. Gao, F. Offi, S. Imada, S. Suga, H. Daimon, and J. Kirschner, *Physical Review B* **71**, 014444 (2005).
 [19] U. Flechsig, F. Nolting, A. Fraile Rodriguez, J. Krespasky, C. Quitmann, T. Schmidt, S. Spielmann, and D. Zimoch, *AIP Conf. Proc.* **1234**, 319 (2010).
 [20] T. Okuda, J. Lobo-Checa, W. Auwärter, M. Morscher, M. Hoesch, V. N. Petrov, M. Hengsberger, A. Tamai, A. Dolocan, C. Cirelli, et al., *Physical Review B* **80**, 180404 (2009).
 [21] C. Chen, N. Smith, and F. Sette, *Physical Review B* **43**, 6785 (1991).
 [22] S. Hufner, *Photoelectron Spectroscopy: Principles and Applications* (Springer, Berlin, 2003).
 [23] M. Morscher, F. Nolting, T. Brugger, and T. Greber, *Manuscript in Preparation* (2011).
 [24] M. Magnuson, N. Wassdahl, A. Nilsson, A. Föhlisch, J. Nordgren, and N. Mårtensson, *Physical Review B* **58**, 3677 (1998).
 [25] J. Osterwalder, T. Greber, A. Stuck, and L. Schlapbach, *Physical Review B* **44**, 13764 (1991).
 [26] J. Wider, F. Baumberger, M. Sambri, R. Gotter, A. Verdini, F. Bruno, D. Cvetko, A. Morgante, T. Greber, and J. Osterwalder, *Physical Review Letters* **86**, 2237 (2001).
 [27] T. Greber, *Journal of Physics - Condensed Matter* **13**, 10561 (2001).
 [28] M. Donath, *Surface Science Reports* **20**, 251 (1994).

- [29] A. Chassé and P. Rennert, *Physical Review B* **55**, 4120 (1997).